BASINS OF ATTRACTION FOR TRIPLE LOGISTIC MAPS

JAN ANDRES AND JIŘÍ FIŠER

Abstract. Attractors and the associated basins of attraction for triple logistic maps are detected and visualized numerically (see [8]) as well as by the technique of critical manifolds due to C. Mira (see e.g., [7],[5]).

1. Introduction

The logistic maps have been often used as a paradigm for demonstrating many nonlinear phenomena like the chaotic behaviour. Moreover, this model is realistic, describing e.g. the population dynamics. In difference to the well-known one dimensional case, planar models have been studied rather rarely (see e.g., [1], [3], [4]). Besides the standard numerical simulations, the "analytical" method of critical curves has been applied for detecting the basins of attraction as well. In R^2, the situation is already very complex. Hence, the natural question arises whether we are still able to analyze such models in R^3 by means of the similar methods. This is the main stimulation and purpose of our paper.

2. Preliminaries

Let us consider the following cases of logistic maps:
Classical logistic map:

$$T_c : x \to \lambda x(1-x),$$

AMS (1991) subject classification: Primary 58F08, 58F12.

Key words and phrases: Logistic maps, basins of attraction, numerical simulations, critical manifolds technique.

Supported by grant no. 311–03–001 of Palacký University, Olomouc.

where λ is a real parameter;

Similar *single* logistic map:

$$T_s : x \to (1-\lambda)x + 4\lambda x(1-x),$$

here and below real λ belongs to interval $[0,1]$;

Two-dimensional analogy—*double* logistic map:

$$T_d : \begin{pmatrix} x \\ y \end{pmatrix} \to \begin{pmatrix} (1-\lambda)x + 4\lambda y(1-y) \\ (1-\lambda)y + 4\lambda x(1-x) \end{pmatrix};$$

Three-dimensional analogy—*triple* logistic map:

$$T_t : \begin{pmatrix} x \\ y \\ z \end{pmatrix} \to \begin{pmatrix} (1-\lambda)x + 4\lambda y(1-y) \\ (1-\lambda)y + 4\lambda z(1-z) \\ (1-\lambda)z + 4\lambda x(1-x) \end{pmatrix}.$$

In difference to T_c, the fixed points of T_s, T_d and T_t are independent on the parameter λ. For the triple logistic map, one can find eight fixed points (see Fig. 1a):

$$\begin{aligned} A &= [0,0,0], \\ B &= [0.75, 0.75, 0.75], \\ C = C_1 &\approx [0.61, 0.19, 0.95], \\ C_2 &\approx [0.95, 0.61, 0.19], \\ C_3 &\approx [0.19, 0.95, 0.61], \\ D = D_1 &\approx [0.41, 0.12, 0.97], \\ D_2 &\approx [0.97, 0.41, 0.12], \\ D_3 &\approx [0.12, 0.97, 0.41]. \end{aligned}$$

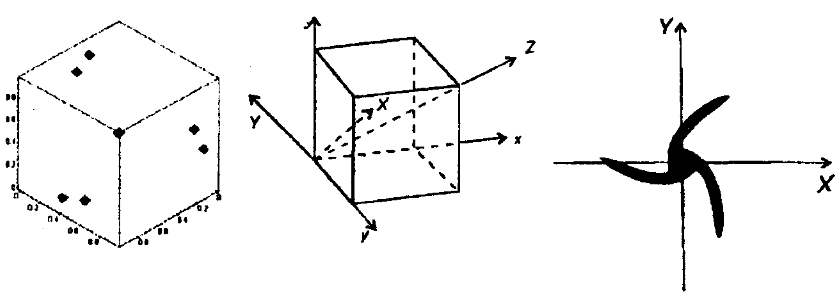

Fig. 1. a) Fixed points, b) new axes and c) triangular symmetry

Points A and B belong to the axis of symmetry Δ (three equal coordinates), C_1, C_2, C_3 and D_1, D_2, D_3 are the vertices of two equilateral triangles (orthogonal to Δ, they belong to planes $x+y+z=const.$). It will be convenient for us to change the axes from a usual (x,y,z)–system to another orthogonal system (X,Y,Z) (see Fig. 1b)) in order to describe projections into plane $x+y+z=const.$ directly in the (X,Y)–plane. By this plotting we can discover the triangular symmetry of our pictures (see e.g. Fig. 1c). For more details concerning the combination of chaos and symmetry see [2]. Hence, to obtain only qualitative properties we can reduce all C_i to C and all D_i to D, $i=1,2,3$.

The simplest attractors in general are attracting fixed points, i.e. when all eigenvalues of the matrix of linearization at the fixed point have modules less than 1.

The Jacobians for the triple logistic map and particularly those at the points A, B, C and D read approximately as follows:

$$J=\begin{pmatrix} 1-\lambda & 4\lambda(1-2y) & 0 \\ 0 & 1-\lambda & 4\lambda(1-2z) \\ 4\lambda(1-2x) & 0 & 1-\lambda \end{pmatrix},$$

$$J_A=\begin{pmatrix} 1-\lambda & 4\lambda & 0 \\ 0 & 1-\lambda & 4\lambda \\ 4\lambda & 0 & 1-\lambda \end{pmatrix}, \qquad J_B=\begin{pmatrix} 1-\lambda & -2\lambda & 0 \\ 0 & 1-\lambda & -2\lambda \\ -2\lambda & 0 & 1-\lambda \end{pmatrix},$$

$$J_C\approx\begin{pmatrix} 1-\lambda & 2.49\lambda & 0 \\ 0 & 1-\lambda & -3.60\lambda \\ -0.89\lambda & 0 & 1-\lambda \end{pmatrix}, \qquad J_D\approx\begin{pmatrix} 1-\lambda & 3.06\lambda & 0 \\ 0 & 1-\lambda & -3.76\lambda \\ 0.69\lambda & 0 & 1-\lambda \end{pmatrix}.$$

Every fixed point has two complex conjugate eigenvalues (*cev*) (they have the same modules) and one real (*rev*). The situation is schematically sketched in the table below, where u denotes a module greater than 1 and s a one less than 1.

λ		0.1	0.2	0.3	0.4	0.5	0.6	0.7	0.8	0.9	1.0
A	*rev*	u	u	u	u	u	u	u	u	u	u
	cev	s	s	u	u	u	u	u	u	u	u
B	*rev*	s	s	s	s	s	s	u	u	u	u
	cev	u	u	u	u	u	u	u	u	u	u
C	*rev*	u	u	u	u	u	u	u	u	u	u
	cev	s	s	s	s	s	u	u	u	u	u
D	*rev*	s	s	s	s	s	s	u	u	u	u
	cev	u	u	u	u	u	u	u	u	u	u

We can see that no fixed points are stable. They generate at least one-dimensional unstable manifold.

So, every other attractor must be more complicated. There are examples of attractors for some values of parameter λ in Fig. 2, represented by projection into the plane (X, Y).

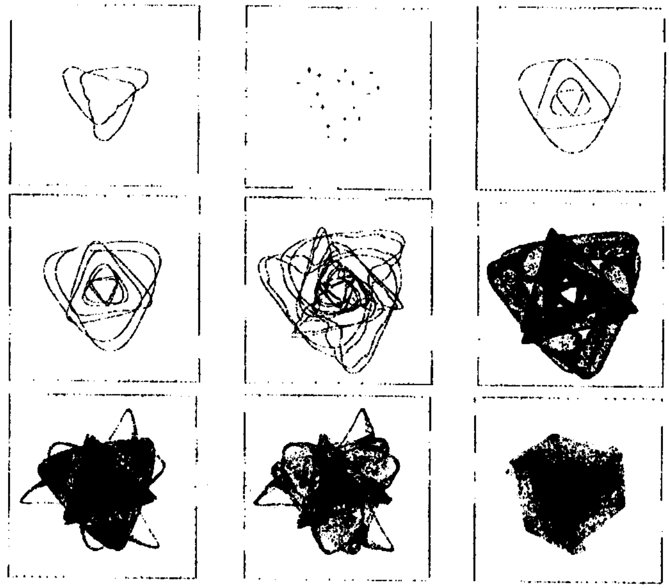

Fig. 2. Examples of attractors for the triple logistic map

It is usually useful to make the bifurcation diagrams of our maps. Such diagrams describe the asymptotical behaviour of maps for a varying parameter. Since the map is 3D and we are able to make only a 1D projections, it is good to create more than one diagram. In Fig. 3, we can see two bifurcation diagrams for a single logistic map (on the left: whole and detailed) and two ones for the triple logistic map (on the right: for coordinates Z and X). We can distinguish the interval of the same behaviour of single and triple logistic maps.

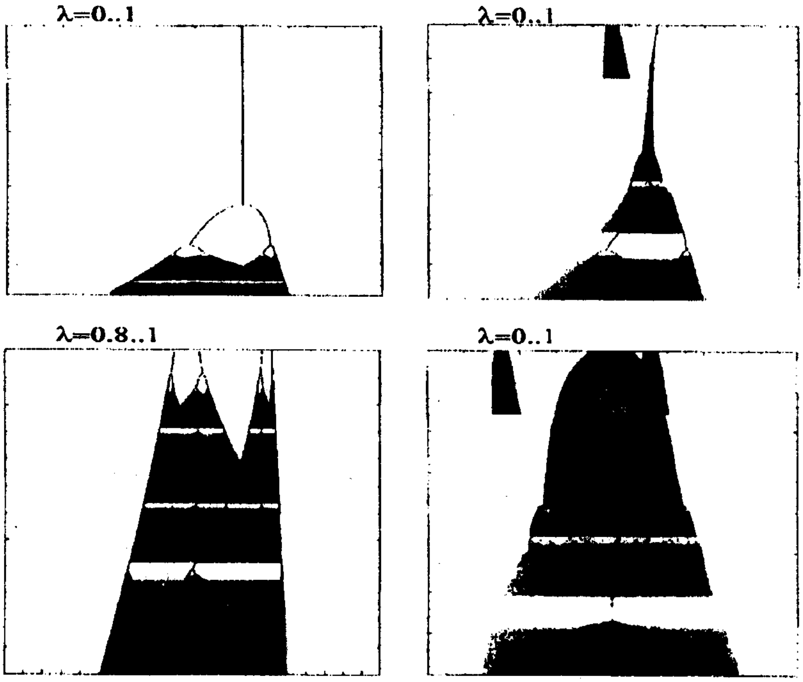

Fig. 3. Bifurcation diagrams for single and triple logistic maps

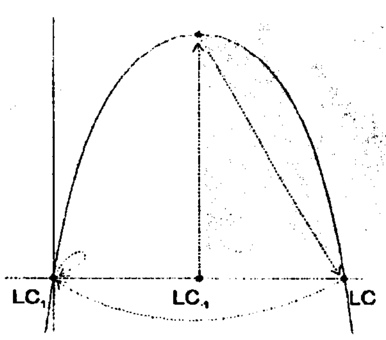

Fig. 4. An example of critical points technique

3. Method of critical surfaces

Critical manifolds

The rigor of the general theory of critical manifolds has been justified in [5]. Here, we need only its brief restriction to differentiable noninvertible maps $T : R^n \to R^n$. *Critical manifold LC* (*critical points* for $n = 1$, *critical* *curves* for $n = 2$ and *critical surfaces* for $n = 3$) is the geometrical locus of points $x \in R^n$, having at least two coincident preimages, located on a manifold LC_{-1}. Since LC_{-1} denotes the locus of the coincident preimages of LC, $LC = T(LC_{-1})$. The LC_{-1} is defined by the equation

$$\det(J) = 0.$$

Further manifolds can be defined by means of the iterates of LC or LC_{-1}, respectively.

$$LC_i = T^i(LC) = T^{i+1}(LC_{-1}), \quad i = 0, 1, 2 \ldots, \quad (LC_0 = LC).$$

The LC divides R^n into the subsets of points with the same number of preimages (see Fig. 4). Analogically, the LC_i is dividing R^n into the subsets of points with the same number of preimages of the $(i + 1)$-rank (i.e., the same number of preimages for the map T^i). Such sequence of manifolds LC_i can define the absorbing set (i.e., the set which cannot be left by any trajectory after reaching it). This procedure is described in Fig. 4 (the single logistic map for $\lambda = 1$) and Fig. 5 (there are examples for the double logistic map with two limit cycles and for a certain quadratic map with a chaotic attractor).

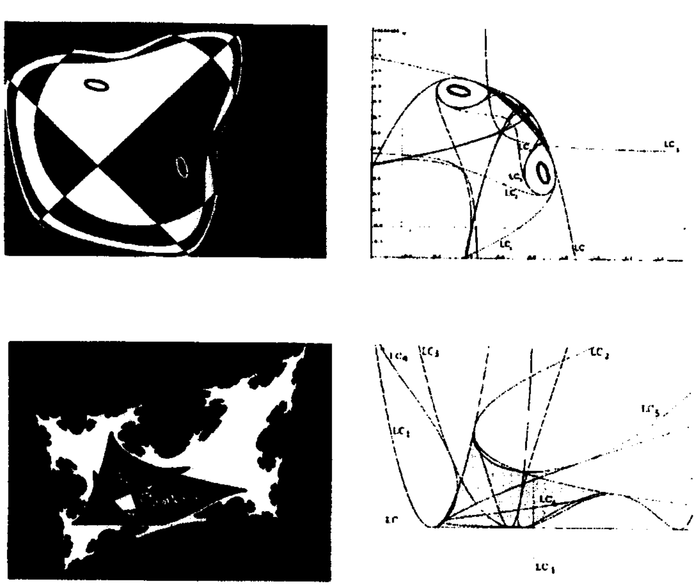

Fig. 5. Examples of critical curves technique

4. Critical surfaces method for the triple logistic map

As one could see above, for definition of LC_{-1}, we must solve the equation

$$\det(J) = \det\begin{pmatrix} 1-\lambda & 4\lambda(1-2y) & 0 \\ 0 & 1-\lambda & 4\lambda(1-2z) \\ 4\lambda(1-2x) & 0 & 1-\lambda \end{pmatrix} = 0.$$

For $\lambda = 1$, the situation is quite simple: the LC_{-1} is formed by three planes

$$x = \frac{1}{2}, \quad y = \frac{1}{2} \quad \text{and} \quad z = \frac{1}{2};$$

the LC by

$$x = 1, \quad y = 1 \quad \text{and} \quad z = 1;$$

the LC_i, $i = 1, 2, 3, \ldots$ by

$$x = 0, \quad y = 0 \quad \text{and} \quad z = 0.$$

Thus, we can obtain the unite cube as an absorbing set (see Fig. 6).

When parameter λ decreases, the situation becomes rather complicated. For example, for $\lambda = 0.9$, we can obtain the following: LC_{-1} is formed by the surface

$$\begin{aligned} z &= \frac{1}{93312}\frac{46657 - 93312y - 93312x + 186624xy}{1 - 2y - 2x + 4xy} \\ &= \frac{1}{2} + \frac{1}{93312(1 - 2y - 2x + 4xy)}; \end{aligned}$$

for LC_i, $i = 0, 1, 2, \ldots$, we are not able to find out such explicit formulas as for $\lambda = 1$. Therefore, we tried to make the numerical iterates of LC_{-1}. Nevertheless, only LC has some practical meaning (see Fig. 7).

5. Numerical explorations

When analytical methods cannot be applied, we try to use the numerical explorations (see [8]). The situation how the basins of attraction are complicated, can been seen in Fig. 8. There are sections of basins of attractions (black) of the associated attractors (white) for some values of parameter λ.

To obtain 3D visualization, we can collect such sections to one picture. The example of such a technique is in Fig. 9, where $\lambda = 0.2$. There are four attractors—limit cycles. The basins of small ones are "hidden" in one big.

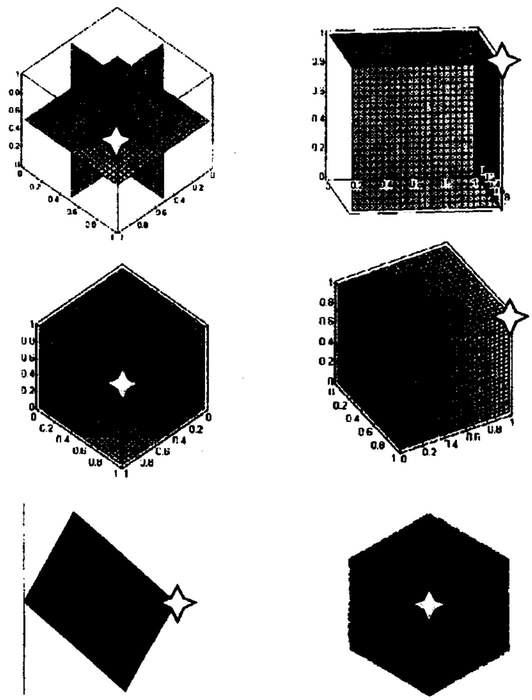

Fig. 6. Method of critical surfaces for $\lambda = 1$: LC_{-1}; LC_0; LC_1; combination of LC_0 and LC_1 (a unite cube); side and front views of numerical results

In Fig. 9, one can see the result of visualization, the attractors, front and back views.

6. Concluding remarks

The main question whether we are able to apply the method of critical manifolds in 3D was affirmatively answered only partially. In other cases, the situation is even more complicated. The numerical explorations seem to be more efficient here. Especially, when the analytical methods depend on computer aided visualizations (see Fig. 6).

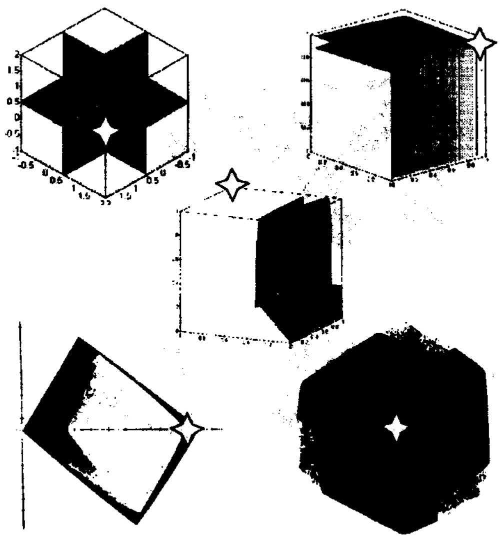

Fig. 7. Method of critical surfaces for $\lambda = 0.9$: LC_{-1}; LC_0; LC_1 (already rather complicated); side and front views of numerical results (in the side view on the left, the attractor is white, while the associated basin of attraction is black)

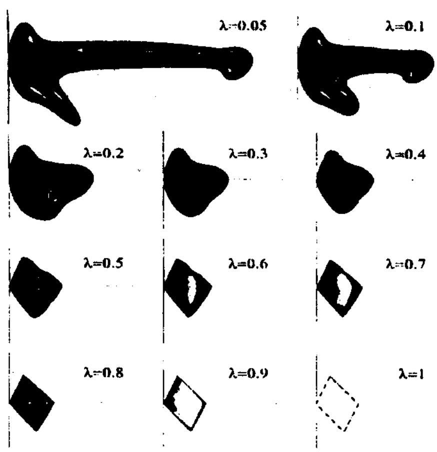

Fig. 8. Sections of basins of attraction for some values of parameter λ (basin of attraction of the main attractor—black, attractors and "subbasins" of attraction of other attractors—white)

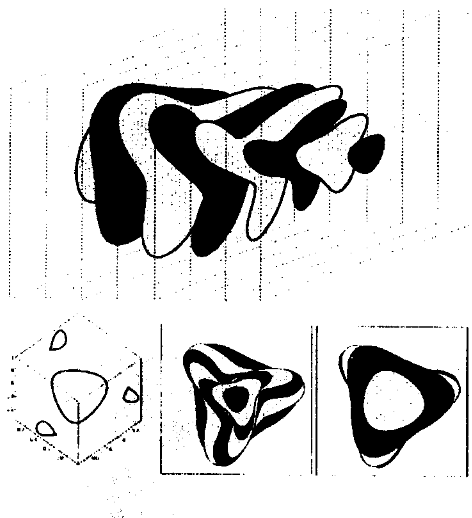

Fig. 9. Visualization of basin of attraction for $\lambda = 0.2$

References

[1] J. Andres, Z. David, *Basin of attraction metamorphoses for two-dimensional endomorphisms*, in Acta UPO, Phys. 35 (1996), 221–251.

[2] M. Field, M. Golubitsky, *Symmetry in Chaos*, Oxford Univ. Press, Oxford 1992.

[3] L. Gardini, R. Abraham, R. J. Record, D. Fournier-Prunaret, *A double logistic map*, Int. J. Bifurcat. Chaos, 4 (1994), no. 1, 145–175.

[4] Yan Gu, Mingwhei Tung, Jian-Min Yuan, Da Hsuan Feng, Narducci, L. M., *Crises and Hysteresis in Coupled Logistic Maps*, Phys. Rev. Letters 52 (1984), no. 9, 701–704.

[5] J. Gumowski, C. Mira, *Dynamique Chaotique*, Cepadnes Editions, Toulouse 1980.

[6] J. Hale, H. Koçak, *Dynamics and Bifurcations*, Springer–Verlag, Berlin 1991.

[7] C. Mira, *Chaotic Dynamics*, World Scientific, Singapore 1987.

[8] H. E. Nusse, J. A. Yorke, *Dynamics: Numerical Explorations*, Springer, Berlin 1994.

[9] E. Ott, *Chaos in Dynamical Systems*, Cambridge Univ. Press, Cambridge 1993.

Dept. of Math. Anal.
Fac. of Science
Palacký University
Tomkova 40
779 00 Olomouc-Hejčín
Czech Republic